Bacterial communities of decaying Norway spruce follow distinct slope exposure and time-dependent trajectories

Maraike Probst,[1†]* [ID] María Gómez-Brandón,[1,2†]
Tommaso Bardelli,[1,3] Markus Egli,[4] Heribert Insam[1]
and Judith Ascher-Jenull[1,3]

[1]*Institute of Microbiology, University of Innsbruck, Innsbruck, Austria.*

[2]*Departamento de Ecología y Biología Animal, Universidad de Vigo, Vigo, Spain.*

[3]*Department of Agrifood and Environmental Science, University of Florence, Florence, Italy.*

[4]*Department of Geography, University of Zürich, Zürich, Switzerland.*

Summary

Deadwood decay employs a complex metabolism and provides carbon and nutrients for soils. Although being highly diverse, the contribution of the bacterial deadwood colonizing community is underexplored compared with the fungal one. Therefore, we performed an *in-field* mesocosm study and monitored the bacterial communities in decaying experimental *Picea abies* wood blocks and their underlying soil on north- and south- exposed slopes in the Italian Alps over a 2-year period. The faster deadwood decay at the south-facing slope was associated with a higher bacterial richness and a higher number of specialist operational taxonomic units (OTUs) which were more strongly correlated to environmental parameters than other bacterial community members. With progressing decay, the wood and soil bacterial communities became more similar in terms of richness, diversity and evenness and especially at the south-facing slope, they also became more similar in terms of community composition. Exposure-specific OTUs suggest wood-soil interaction. However, despite the strong influence of exposure on the soil bacterial communities, the *P. abies* wood blocks shared a comparably high number of OTUs with the soil irrespective of the slope. At finer taxonomic scale, we identified *Pseudomonas, Microbacteria, Sphingomonas, Xanthomonas, Methylovirgula* and *Burkholderia* as decay associated, although their functional role needs further studies.

Introduction

Deadwood decay is essential for the functioning of forest ecosystems (Stokland *et al*., 2012) and understanding its underlying mechanisms, that is its dynamics, the decomposing organisms involved and the impact of environmental conditions, is crucial and of global ecological and forest-economic relevance (Garbarino *et al*., 2015; Stutz and Lang, 2017). Deadwood provides shelter and nutrition to a wide range of saproxylic organisms and it largely influences the global forest carbon (C) balance acting as a temporal store estimated at 73 Pg C (Pan *et al*., 2011). Moreover, there exists evidence of complex fungal-bacterial interactions, both positive and negative, within the deadwood environment, even though, the identity and ecology of bacterial communities in decaying wood remains underexplored compared with fungi which are supposed to be the main deadwood decomposers (Valášková *et al*., 2008; Sun *et al*., 2014; Hoppe *et al*., 2015; Hervé *et al*., 2016; Johnston *et al*., 2016; Kielak *et al*., 2016; Rinta-Kanto *et al*., 2016; Tláskal *et al*., 2017).

Several factors were found to govern the composition of deadwood-inhabiting bacteria such as the stage of wood decay, with a higher bacterial abundance and richness at advanced stages of wood decay (Hoppe *et al*., 2015; Gómez-Brandón *et al*., 2017); the host tree species and the forest management regime (Hoppe *et al*., 2015); the physico-chemical properties of the wood, particularly the remaining mass, density, pH, water content and C:N ratio (Hoppe *et al*., 2015); and the soil type (Sun *et al*., 2014). The latter authors observed that the bacterial assemblage in experimental wood blocks from Norway spruce [*Picea abies* (L.) Karst] was closely related to the microbial community from the underlying soil, which suggests an edaphic origin of saproxylic bacteria or an
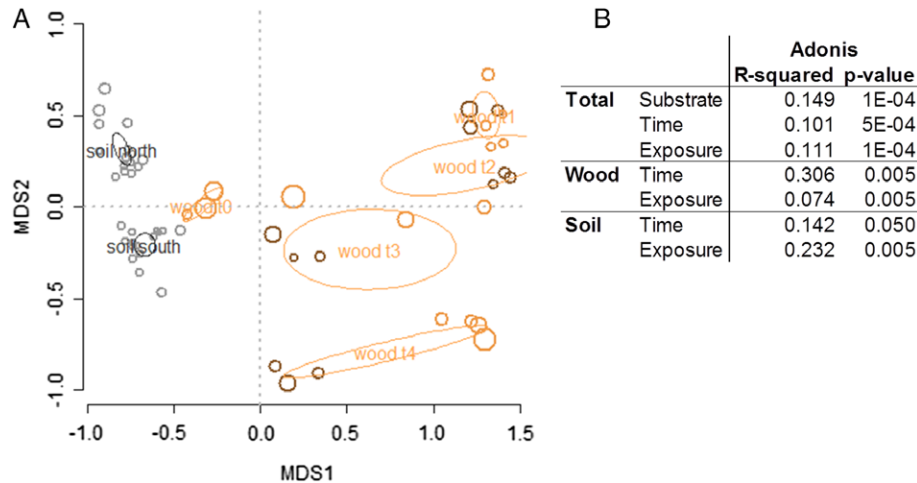
Fig. 1. A. Non-metric multidimensional scaling (NMDS) of bacterial community data obtained by Illumina Miseq profiling based on Bray Curtis similarity. Stress = 0.076 (R^2 = 0.924). Site scores were coloured as follows: light grey = soil, brown = deadwood; light colours = north-exposure, dark colours = south-exposure. The radius of the circles correlates to the accuracy of component prediction. Ellipses embracing sample groups were drawn at a confidence level of 95% around group centroid for north- and south-exposure for soil samples, and decay time for deadwood samples (t0 = 0 weeks, t1 = 12 weeks, t2 = 25 weeks, t3 = 52 weeks, t4 = 104 weeks). B. Effect of the experimental factors (substrate, time and exposure) on the distances between samples according to Adonis analysis. The *R*-squared might be interpreted as size effect of the respective factor while the *p*-value indicates the significance of such effect. [Color figure can be viewed at wileyonlinelibrary.com]

indirect influence of the soil environment, for instance via alteration of the fungal community within deadwood.

Topographic features, particularly the slope exposure, may also affect the deadwood decay process as recently shown by Fravolini and colleagues (2016) during a 2-year field mesocosm monitoring of *P. abies* wood decay along an altitudinal gradient ranging from 1200 to 2000 m above sea level (a.s.l.) in the Italian Alps. These authors registered faster decay rates at the north-facing slopes than at the south-facing ones up to an elevation of 1800 m a.s.l., due to the higher moisture and weathering of the soils (higher clay minerals content) along with a lower pH - favourable conditions especially for fungi – at northern slopes. Nonetheless, at sites above 1800 m a.s.l. moisture does not seem to be a limiting factor, and consequently temperature appears to play a more prominent role leading to faster decay rates at south-facing slopes (Egli *et al.*, 2016; Fravolini *et al.*, 2016). However, little attention has been paid to bacteria in this study area. The aim of the present study was to analyse the bacterial community composition under the same experimental conditions as Fravolini and colleagues (2016) by using Illumina MiSeq sequencing in order to: (1) determine the exposure-effects (north- vs. south-facing slope) on the bacterial communities involved in the decay of *P. abies* wood blocks and the underlying soil at an elevation of 2000 m a.s.l. (cold environment, relatively close to the treeline); (2) identify bacterial groups, known as potential key players in *P. abies* wood decay, at a finer taxonomic scale.

We hypothesised that bacterial diversity and richness in *P. abies* wood blocks and soil would be higher at the

south- than at the north-facing slope considering the warmer and less acidic conditions at south-exposure. As the wood's integrity decreases with progressing decay, offering a higher surface area and a higher nutrient variety, more niches become available for microbial colonization which can potentially be colonized by microbes present in the surrounding soil. Therefore, we expected higher similarities in bacterial community composition between *P. abies* wood blocks and the underlying soil as a function of progressing wood decay.

Results and discussion

Bacterial communities of P. abies wood blocks and the underlying soil clustered separately and as a function of both exposure and time

Illumina analysis yielded a total of > 4.4 million reads and the bacterial community composition of each of the 57 samples was represented by 30 001 reads after subsampling. The sequences were clustered into 10 411 different OTUs at 97% similarity. By sampling OTUs and estimating Chao richness, rarefaction curves were not fully saturated (Supporting Information Fig. S1) while they reached full saturation sampling for the Shannon index.

Both the *P. abies* wood blocks and the underlying soil showed distinct characteristics regarding their bacterial community composition and abiotic parameters (Fig. 1A, Supporting Information Figs. S2 and S3). Taking into account that the observation period focussed on early wood decay (up to 104 weeks, t4), the detected cellulose and especially lignin degradation rates were small

(Fravolini *et al*., 2016) (Supporting Information Fig. S6). In spite of this fact, the bacterial community composition in the wood underwent major changes (Fig. 1A). While the soil bacterial community mainly differed depending on the slope exposure, the deadwood community followed an exposure-dependent time trajectory. Comparing centroid distances in the ordination using Adonis analysis (Fig. 1B), 31% of the explained variance was attributed to the time factor separating the earlier (t1 and t2) and the later (t3 and t4) stages of initial wood decay (p = 1e-4). This time trajectory of wood decay was also influenced by the slope exposure (p = 1e-4) and even though the overall effect size was small (7.4% variance), the interaction between time and exposure clearly separated the wood samples in the later decay stages (Fig. 1A). When the community data were transformed into a presence-absence matrix, the clustering was preserved (*data not shown*). Here, the size effect of exposure (11% variance) on the ordination was comparable to the time effect (10% variance). The observed clustering was confirmed when detrended analysis was applied and rare species were downweighted (Supporting Information Fig. S4), indicating that not only rare species and differential abundances were responsible for the differences observed.

The fresh wood blocks (t0) clustered closer to the soil in terms of bacterial community composition than to the more decayed ones (Fig. 1A). The wood blocks were collected from one representative *P. abies* tree in the study area, and as such could have been in contact with the forest soil during felling and cutting. As freshly cut wood is dense, the high similarity to soil was probably due to the presence of soil bacteria on the wood surface. Therefore, the bacterial community of the wood blocks at t0 may not be exclusively representing the actual wood degrading community. To avoid misinterpretation, t0 was kept as an individual time point distinct from early (t1 and t2) and later (t3 and t4) sampling points.

In order to gain a deeper insight into the different composition of the bacterial communities in the wood blocks and their underlying soil at the early and late time points and at the north- and south-exposed slope (Fig. 1A), both the presence/absence and the abundance of taxonomic groups was investigated in more detail. The majority of sequences were annotated as Proteobacteria (Supporting Information Fig. S5), which is in line with previous studies on *P. abies, Fagus sylvatica* and *Pinus sylvestris* wood decay (Valášková *et al*., 2008; Sun *et al*., 2014; Hoppe *et al*., 2015; Hervé *et al*., 2016; Kielak *et al*., 2016; Rinta-Kanto *et al*., 2016) and with other wood decay associated environments such as leaf litter (Tláskal *et al*., 2016). Furthermore, Acido- and Actinobacteria were also found in high richness and abundance (Supporting Information Fig. S5). Actinobacteria are known to play a key role in the early colonization and decay of deadwood logs

(Hoppe *et al*., 2015), and the low pH in decaying wood might explain the predominance and high OTU variety of Acidobacteria as wood-associated bacteria (Valášková *et al*., 2008; Kielak *et al*., 2016) (Supporting Information Fig. S5). Also Planctomycetes were present in relatively high abundances (Supporting Information Fig. S5), accounting for 11% of all reads in the wood samples and for 12% of all reads in soil samples, respectively (Supporting Information Fig. S5), which has been observed before in decaying *P. abies* (Fagervold *et al*., 2014; Sun *et al*., 2014). In addition, several Planctomycetes OTUs were found to be unique for one sample group, e.g. in either wood or soil, at either north- or south-exposed samples or at only t0, early (t1 and t2) or later (t3 and t4) time points of deadwood decay. However, the role of Planctomycetes in deadwood decay remains unclear.

Figure 2 lists all OTUs of the dataset according to their taxonomic annotation on the y-axes (Fig. 2A–E). The categorical x-axis indicates by colour whether an OTU was found specifically in wood or soil (first bar in each panel), at north- or south-exposure (second bar of each panel) or at the early or later stages of initial deadwood decay (third bar of each panel). An OTU was considered affiliated to a certain substrate, time or slope exposure if it was detected solely in the samples of this group (unique OTUs) or if it was differentially overrepresented as identified by LEfSe (p-value < 0.05, lda > 2; Segata *et al*., 2011). In all of the core phyla, OTUs with a specialized affiliation were observed (Fig. 2A–E). These were not only members of the rare biosphere, but also abundant OTUs, that is, with high read count (> 0.5% of all reads). These OTUs were often detected across sample groups and can be seen as generalist species that can thrive under a broad spectrum of environmental conditions (Pandit *et al*., 2009). A number of 13 abundant, generalist OTUs were found in all of the samples across all time points and were differentially abundant in the wood blocks as a function of decay (Supporting Information Fig. S5C). Abundant Actino- and Acidobacteria OTUs mainly appeared in the earlier time points (up to 25 weeks) confirming that Actinobacteria are among the dominant early wood colonizers as pointed out by Hoppe and colleagues (2015). Smaller unique and characteristic OTUs, however, were found more frequently at later time points (Fig. 2B and C). Many Proteobacteria OTUs, including some abundant Proteobacteria OTUs, were unique or overrepresented at the later decay stages, especially at the south-facing slope (Fig. 2; Supporting Information Fig. S5), despite the decreasing tendency of Proteobacteria abundance over time (Supporting Information Fig. S5C). Unique and characteristic Planctomycetes OTUs were predominantly found in the soil samples compared with a lower number in the wood
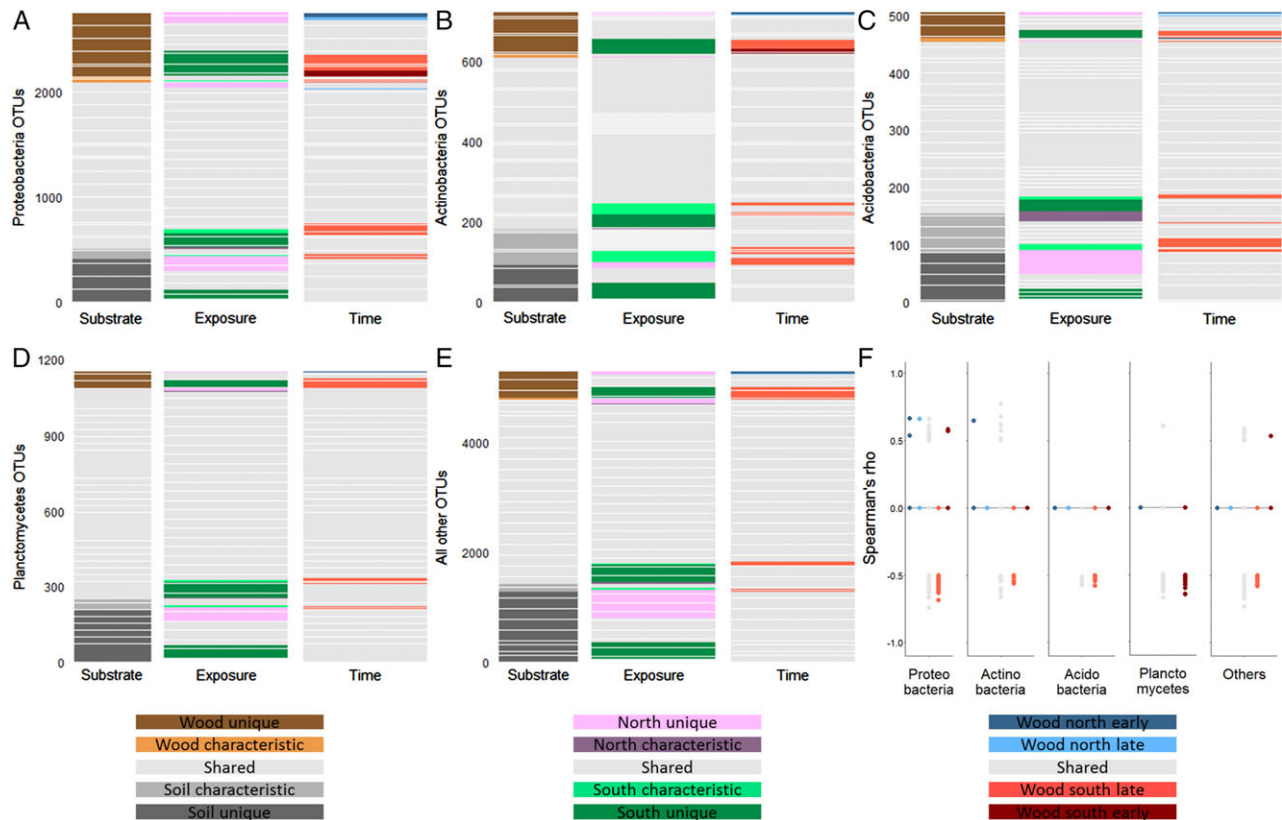
Fig. 2. A–E. OTU occurrences during *P. abies* wood decay and the underlying soil at the north- and south-facing slopes over time. The overall bacterial community across all samples was subdivided by taxonomic annotation. The y-axis indicates the number of OTUs within the respective taxonomic group while the categorical x-axis illustrates whether this OTU was unique, characteristic or not specifically associated with a substrate (soil vs. wood), north- vs. south-exposure or sampling time [initial t0, early time points (12, 24 weeks), later time points (52, 104 weeks)]. *Unique* was defined as exclusively found within samples of this group and *characteristic* was defined as significantly overrepresented in one sample group as determined by linear discriminant analysis size effect (LEfSe) algorithm (Segata *et al.*, 2011) (LDA > 3, *p* < 0.05). F. Relation of OTUs to environmental variables. The distribution of correlation coefficients (|r| > 0.5) between the abundances of OTUs present in at least three wood samples and the environmental variables moisture content, cellulose content and pH is displayed. Colours associate the correlating OTU to a certain time point or slope exposure. The correlation coefficients were summarized over all environmental variables as the phylum annotation of the correlating OTU and not the specific environmental variable affected the strength of the correlation or its directionality (Supporting Information Fig. S8). [Color figure can be viewed at wileyonlinelibrary.com]

blocks. While unique OTUs were mainly present in the north-exposed soil (Fig. 2D), around half of the Planctomycetes OTUs unique to wood were only found at the south-facing slope in the later stages of decay. Planctomycetes constitute a deep branching lineage of the bacterial phylogenetic tree and are known for their genome variability and cell compartmentalization (Youssef and Elshahed, 2014). In addition to their reported lignolytic potential (DeAngelis *et al.*, 2011), these special features might support their establishment in a variety of ecosystems and ecological niches, probably also able to perform unique functions.

Emphasizing the complexity of the *P. abies* wood blocks and the underlying soil bacterial communities, the hierarchy of phyla by number of OTUs was unaffected by both time and exposure (Supporting Information Fig. S5A–C). Nevertheless, a total of 2067 OTUs were unique for soil and 1306 unique for wood. The taxonomic

distribution of these unique OTUs differed as a function of decay time and slope exposure (Fig. 2, Supporting Information Fig. S5D). While at the north-facing slope the number of unique OTUs in the wood samples decreased from 84 to 56 with progressing decay, their number increased from 78 to 404 at the south-facing slope (Fig. 2). These unique OTUs might be seen as specialists which need specific habitat conditions to survive and potentially play key roles in terms of ecosystem functioning. This could be an indication that niche-based mechanisms rather than stochastic processes are driving the bacterial community composition at the later decay stages and primarily at the south-facing slope. This is achieved by selecting specific microbial groups based on their ability to inhabit and exploit new niches available over wood decay progression as pointed out by Kielak and colleagues (2016). Moreover, the distribution of unique and characteristic OTUs across several phyla,
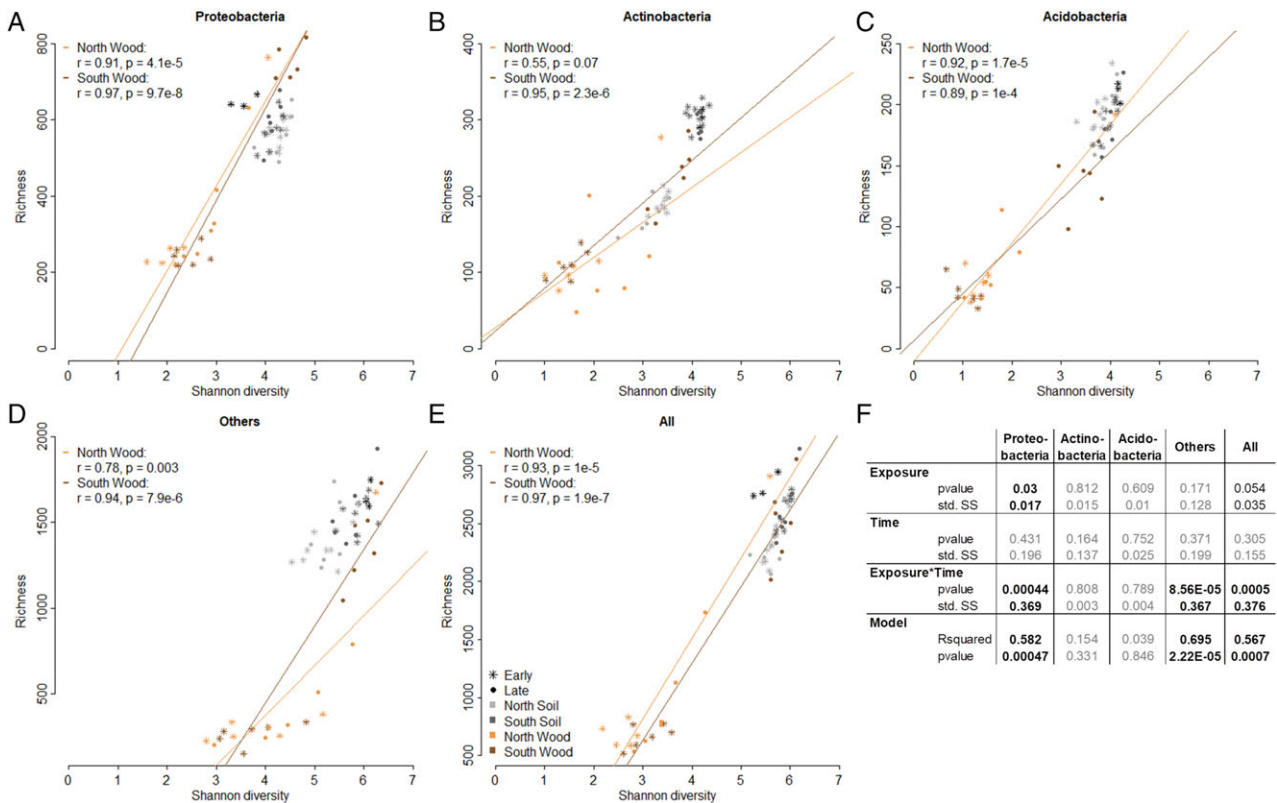
Fig. 3. Correlation between richness and Shannon diversity of OTUs belonging to Proteobacteria (A), Actinobacteria (B), Acidobacteria (C), all other bacterial phyla (except Proteobacteria, Actinobacteria and Acidobacteria) (D) and all OTUs (E). By definition, richness and Shannon diversity of a given community are linearly dependent. Fresh (not decayed) wood blocks (t0) are indicated as black stars. The coloured lines present the visualization of the linear correlation of richness and Shannon diversity for north- and south-exposed slopes and the correlation statistics are given in each panel. (F) Model specifications estimating the effect of the time and the exposure on the ratio of richness and diversity of the overall bacterial community (E) and the respective taxonomic groups displayed in (A–D). SS: Sum of squares. For each bacterial group (A–E), one model was calculated and the effect size of the factor (time, exposure and time × exposure) was standardized to the total sum of squares. [Color figure can be viewed at wileyonlinelibrary.com]

especially at the later stages of decay (Fig. 2), indicates that several functional niches become available to bacteria during the process of deadwood decay, assuming a connection between the functional potential of an organism and its taxonomy.

South-exposed P. abies wood blocks were characterized by higher bacterial richness and diversity and by a higher similarity to the underlying soil

Although the taxonomic distribution at phylum level was comparable among all of the samples (Supporting Information Fig. S5), soil samples were more diverse (mean Shannon index = 5.77) and had a higher OTU richness (mean richness = 2473 OTUs) compared with the *P. abies* wood blocks (mean Shannon index = 4.04, mean richness = 1462 OTUs) (see also Fig. 3). The faster wood decay rates (decay constant rates: north = 0.003 ± 0.016 y^{-1}; south = 0.046 ± 0.028 y^{-1}) found at the south-facing slope at such altitudes (Supporting Information Fig. S6; Fravolini *et al.*, 2016) were accompanied by higher bacterial community richness and diversity than at the

comparable north-facing slope (richness = 930 OTUs, Shannon index = 5.82; Fig. 3). In fact, at south-exposure the bacterial richness and diversity in the wood blocks (Shannon index = 3.42, richness = 2519 OTUs) were comparable to the underlying soil at the later decay stages. This is consistent with a previous study on *F. sylvatica* from Hoppe and colleagues (2015) and on *Abies faxoniana* from Chang and colleagues (2017) in which they observed that bacterial richness potentially increases as decay progresses. Moreover, it is also in line with previous findings on fungal species richness on *P. abies* logs obtained by 454 pyrosequencing where the fungal community in wood becomes increasingly species rich along the decay gradient and more similar to fungal communities in soil (Mäkipää *et al.*, 2017).

Both measures, diversity and richness, are known to positively affect ecosystem stability: The more diverse, the less sensitive is an ecosystem to environmental changes (Lynch *et al.*, 2004). An additional characteristic found tightly related to ecosystem stability is evenness (Wittebolle *et al.*, 2009; Mikkelson *et al.*, 2011; Thibaut *et al.*, 2013) which indicates the distribution of species'

abundances within an ecosystem. Irrespective of the slope exposure, soil samples showed a higher evenness (Pielou's index = 0.738) compared with the *P. abies* wood blocks, in which evenness strongly increased with progressing decay (Pielou's evenness index on average = 0.461 and 0.624 at early and late decay stages, respectively) as also observed for leaf litter decay (Tláskal *et al.*, 2016). Moreover, in terms of exposure the south-facing slope was characterized by a more even bacterial community than the comparable north-facing one (Pielou's index = 0.609 and 0.520 at south- and north-exposure, respectively). Taken together the results of community richness, diversity and evenness, the soil might be interpreted as the more stable environment in terms of bacterial community composition while the wood ecosystem increased stability over time and such increase was more pronounced at the south-facing slope. Another indicator for community stability was the homogeneity within the bacterial communities of sample groups as estimated using betadisper analysis, which can be interpreted as an equivalent for Levene's test of the equality of variances. The homogeneity of the soil bacterial communities was lower compared with the wood community (p = 0.001 on 999 permutations). The homogeneity of the wood bacterial communities followed an interaction effect and increased from north- to south-exposure and from early to late decay stages (p = 0.002 on 999 permutations).

The relation of richness and diversity was linear when all the bacterial phyla were considered (Fig. 3A); as well as when the phyla Proteo-, Acido- and Acidobacteria were considered separately (Fig. 3B–D), or excluded from the total bacterial community (Fig. 3E). Modelling the effect of both the time and the exposure on the ratio of richness and diversity, neither of them had a significant effect on the phyla of Actino- and Acidobacteria (Fig. 3B, C, and F). The independence of Acido- and Actinobacteria richness-diversity ratio with regard to the time and the exposure might suggest a lower dependency of members of these two phyla from organisms belonging to the other bacterial phyla and/or a lower sensitivity of these phyla to environmental changes during wood decay. The latter might point toward Acido- and Actinobacteria occupying more general niches within the deadwood habitat which are less frequently available at the north-facing slope owing to lower decay rates (Supporting Information Fig. S6). This is in line with the fact that members of these phyla are known to possess enzymes involved in the breakdown of cellulolytic material (Lladó *et al.*, 2016) which are relevant throughout all stages of deadwood decay. Brown and Chang (2014) also found evidence of bacteria, that is, *Actinobacterium amycolatopsis* sp. 75iv2, with lignin-decomposing abilities. Interestingly, the presence and the differential abundances of Actinobacteria OTUs observed

in the soil samples as a function of exposure (Fig. 2B, Supporting Information Fig. S5B, C) were also accompanied by differences in richness and diversity (Fig. 3B). This might result in a differential colonization of north- versus south-exposed wood samples that ultimately affect the dynamics of deadwood decay. However, further experiments are needed to provide a more detailed and mechanistic picture.

Nevertheless, the ratio of richness and diversity for Proteobacteria, as well as for the overall bacterial community was strongly influenced by the time and the exposure (Fig. 3A and D–F). This strong interaction effect underlines the relevance of the diverse and rich community, especially of Proteobacteria, for deadwood decay, considering the faster decay observed at the south-facing slope. Interestingly, the sole effect of the decay time was insignificant for all of the models calculated (Fig. 3F). This consistent ratio of richness and diversity over time suggests that the ecosystems at both the north- and the south-facing slopes are functioning ecosystems with different dynamics of deadwood decay.

Overall, the bacterial community of the initial wood blocks (t = 0) shared more observations with the soil samples, especially from the south-facing slope, than with the other wood samples (Fig. 4A and B; see also Fig. 1) (p < 4e-15). At the earlier stages of wood decay (up to 25 weeks), the bacterial community of the *P. abies* wood blocks was quite unique and shared the lowest number of OTUs with the soil and the wood samples with higher degree of decay (Fig. 4) (p = 4e-4). Despite being more diverse, the bacterial community of the south-exposed early wood samples had a lower number of shared observations with the other sample groups compared with its northern counterpart (Fig. 4) (p = 1.3e-14). Nevertheless, the number of shared observations largely increased in the south-exposed wood samples at the later sampling points (Fig. 4B) (p < 2e-16). Taken together, these findings link a more diverse bacterial community with a higher number of specialist OTUs to faster deadwood decay rates at the south-facing slope.

Supporting the potential role of wood-soil interaction suggested by Sun and colleagues (2014), our wood samples shared a comparable number of OTUs with the underlying soil at both slopes (Fig. 4). This could indicate that (1) at the initial stage common soil bacteria are entering the wood blocks and only with progressing decay a specialized community evolves; (2) saproxylic bacteria thriving on deadwood at the latest stages are colonizing the soil especially when dry conditions, as found at south-facing slopes, facilitate aerial spreading. This contributes to the high number of saproxylic bacteria in the soil, which accounted for ~ 70% of the total soil bacterial community (Fig. 4C). In addition, OTUs unique for the north- and the south-facing slope that were not detected in the wood blocks at t0 were found

Fig. 4. Development of bacterial communities during *P. abies* wood decay as shared observations between sample groups (wood, north soil and south soil). A, B. Shared bacterial OTU observations between deadwood and soil samples as well as between deadwood samples were displayed. Error bars illustrate standard deviation. From left to right, the charts display the estimated shared observations of deadwood samples collected at the north- and the south-facing slopes respectively. Categorical time points are as follows: *t0* = time point zero, *early* = wood samples collected after 12 and 25 weeks, and *late* = wood samples collected after 52 and 104 weeks (as in agreement with Fig. 1). C. Shared and unique observations between sample groups as numbers of OTUs. [Color figure can be viewed at wileyonlinelibrary.com]

Site \ Sample	Soil	Shared	Wood
North	781	1113	171
Core	706	8426	1279
South	498	1594	535
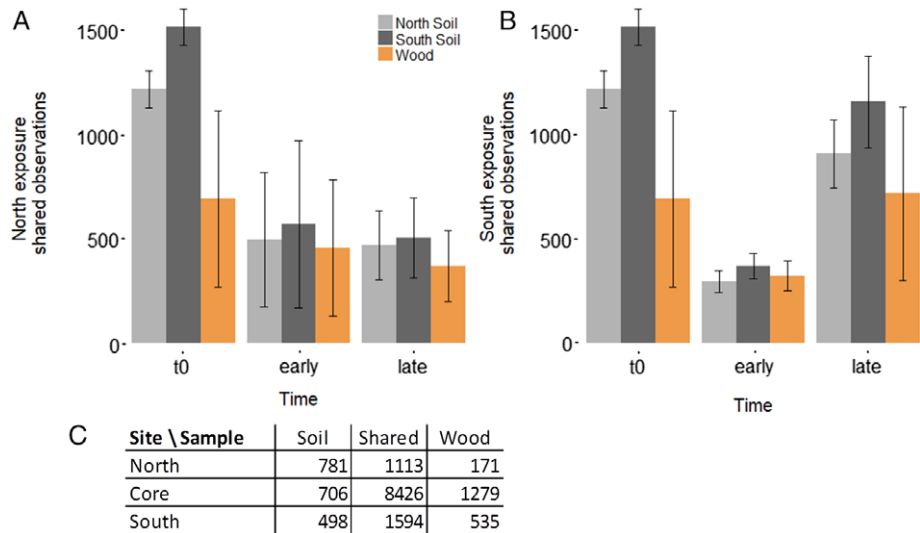
in both soil and wood samples at the early (12 and 25 weeks) and later stages (54 and 104 weeks) of sampling (Fig. 4C). This supports the concept that slope-dependent environmental conditions and soil community composition determined to some extent the bacterial community composition in the deadwood. These findings corroborate the hypothesis of Baas Becking (1931) that *everything is everywhere but the environment selects* (see also Beijerinck, 1913; Nagler *et al*., 2016) (Fig. 4C).

Environmental parameters differentially affected wood bacterial communities

In order to link bacterial community composition and colonization to the physico-chemical characteristics of the *P. abies* wood blocks (Supporting Information Fig. S4), a linear model was calculated. The distinct clusters observed in the NMDS ordination (Fig. 1A) were correlated to the environmental characteristics measured in the same wood blocks by Fravolini and colleagues (2016) using bioenv (rank correlation) and envfit (linear assumption) functions in R (vegan). Moisture, pH and cellulose were chosen as explanatory model variables given their importance in wood decay dynamics as shown in Fravolini and colleagues (2016). Cellulose content was correlated to pH ($r = 0.52$, $p = 0.0052$) and moisture content ($r = 0.61$, $p = 0.0008$) respectively. Although these correlations violate the assumption of linearly independent variables, they are unlikely to interfere with the conclusion whether or not the environmental variables have an impact on the bacterial ordination. Both approaches (bioenv and envfit) confirmed that differences in bacterial community composition could be explained to some extent by moisture, cellulose and pH. The moisture content of the wood samples had the largest effect on the

ordination (envfit $r^2 = 0.48$, $p = 0.001$), followed by the cellulose content (envfit $r^2 = 0.39$, $p = 0.001$). The fact that moisture, cellulose and pH were covariates disabled a precise and accurate estimation of the size effect. Still, the differences in envfit r^2 indicated a stronger effect of the moisture than the cellulose content. The impact of wood pH was smaller (envfit $r^2 = 0.33$, $p = 0.017$), and when investigated by bioenv function it did not improve the model. This is in agreement with the findings from Hoppe and colleagues (2015) who also found that pH did not substantially explain the shifts of the relative abundances of the dominant bacterial phyla irrespective of the tree species (*P. abies* and *F. sylvatica*).

There is evidence for a close fungal-bacterial interaction within the deadwood environment as recently reviewed by Johnston and colleagues (2016). The abundance of fungi, inferred from fungal 18S rRNA gene abundances obtained by real-time PCR (qPCR; Bardelli *et al*., 2017), was much higher in wood compared with soil samples ($\text{mean}_{soil} = 9.6e8$ copies $g_{dry\ weight}^{-1}$, $\text{mean}_{wood} = 1.2e11$ copies $g_{dry\ weight}^{-1}$, $p = 1.9e\text{-}10$). Furthermore, it increased by two log-folds in the wood blocks from t0 ($\text{mean}_{t0} = 3.1e9$ copies $g_{dry\ weight}^{-1}$, $p = 0.004$) to the early time points of wood decay and remained stable until the end of the observation period (104 weeks) (Supporting Information Fig. S7). No significant differences in fungal abundances as measured by 18S rRNA gene copy numbers were found between north- and south-exposure. This underlines the relevance of bacterial deadwood decomposers already at the early stage of decay (up to 104 weeks), because the compositional changes in the bacterial community correspond to the increased decay rates at south- compared with north-exposure. Moreover, no significant impact of the fungal abundance on the bacterial community was found (envfit $r^2 = 0.018$, $p = 0.769$). Assuming a

dependency of the deadwood-inhabiting bacteria on the fungal deadwood decomposers, one would expect the fungal abundance to influence the bacterial community composition. In combination, the absence of such an effect, no exposure difference in fungal abundances and the observed differences in bacterial community composition may suggest that bacteria, independent of fungal colonization, are substantially involved in deadwood decay. It is possible though that the metabolic activity of the colonizing fungi differed between sample groups. However, Mäki-pää and colleagues (2017) reported low nitrogen content in the decaying wood and although they found nitrogen transport into the wood during late decay stages using stable isotope probing, no significant nitrogen transportation was detected during the initial decay stage. The supposedly limited nitrogen availability in the early decay stages of deadwood supports both the unchanged fungal abundances and the important role of bacteria. Further studies, especially involving fungal and bacterial (enzymatic) activities are needed to explore the differential and combined contributions of bacteria and fungi in deadwood decay.

In order to support the differential behaviour of the main phyla (Fig. 2A–E) and to pinpoint those bacterial groups potentially playing a key role in *P. abies* wood decay, all OTUs detected in at least three wood samples were correlated to moisture content, cellulose content and pH (Fig. 2F, Supporting Information Fig. S8). Out of 8344 OTUs detected in the wood samples, 517 OTUs were correlated ($|r| > 0.5$) to one of the three previously mentioned environmental parameters. Interestingly, the strength and the directionality of the correlation were comparable across the environmental variables, but differed among phyla (Fig. 2F, Supporting Information Fig. S8). A number of 104 OTUs were unique to wood of which 53 were only found at the south-facing slope at the later decay stages. Furthermore, there were 91 OTUs unique to south-exposure which correlated to at least one of the studied environmental variables, while those OTUs characteristic for north-exposure were uncorrelated. In conclusion, this supports that environmental conditions partially determined the bacterial community assemblage in the *P. abies* wood blocks associated with faster cellulose decay at the south-facing slope, which is in line with the aforementioned niche-based mechanisms proposed by Kielak and colleagues (2016).

Bacterial community members were correlated more frequently in south- than in north-exposed P. abies wood blocks

Correlation networks on different coefficient thresholds were complex (Supporting Information Fig. S9) and OTUs correlated strongly within and across phyla. Out of the 8861 OTUs appearing at least in three samples of the dataset, 5554 OTUs had at least one correlation with another OTU above $|r| = 0.8$ (Supporting Information Fig. S10). Additionally, more than 75% of all correlations above 0.5 were positive and there were no negative correlations with $|r| > 0.71$. This suggests that the bacterial community associated with *P. abies* deadwood decay was quite interconnected and bacteria were associated with each other. Interestingly, at the south-facing slope, none of the OTUs characteristic for the wood samples in the later decay stages were negatively correlated strengthening the potential relevance of bacterial interactions in deadwood decay at this slope.

The unique or overrepresented OTUs in the *P. abies* wood blocks were less integrated into the network at the north-facing slope (12 and 33 OTUs at early and later stages, respectively) than at the south-facing one (27 and 462 OTUs at early and later stages, respectively) (Supporting Information Fig. S5). Indeed, an OTU characteristic for north-exposure had a lower number of correlation partners in comparison with an average characteristic OTU from south-exposure (mean$_N$ = 16 partners/992 average richness$_N$, mean$_S$ = 89 partners/1594 average richness$_S$, p = 1.5e-5). Along with a higher number of specialist OTUs at the south-facing slope, the connectivity of characteristic OTUs increased from the early to the later decay stages (p = 0.0076) (Supporting Information Fig. S9). This emphasizes that probably both environmental conditions and bacterial interactions influenced initial *P. abies* deadwood decay and raises the question to what extent these two driving forces are interconnected.

A variety of bacteria were identified as potential key players in P. abies deadwood decay

An in-depth look at the taxonomic classification of OTUs in the *P. abies* wood blocks was performed considering: (i) characteristic OTUs from the north- and the south-facing slopes at early and later decay stages (unique or overrepresented as identified by LEfSe and detected in at least three independent samples); (ii) OTUs correlated to at least one of these characteristic OTUs ($r > 0.8$); (iii) abundant OTUs (read abundance > 0.5% of all reads in the dataset); (iv) highly connected OTUs (> 100 connections in the correlation network) and (v) OTUs correlated to an environmental parameter with influence on the bacterial community profile (moisture, cellulose and pH). In sum, there were 1754 OTUs, the majority of which were unclassified at genus level and 125 unclassified at phylum level. The full list can be found in Supporting Information Table S1.

Four OTUs were repeatedly identified as potential key players by high read abundance, high correlation to the studied environmental parameters and overrepresentation in the wood blocks at the earlier time points (up to

25 weeks) independent of the slope exposure. They were classified as *Microbacteriaceae* (Actinobacteria), and members of the Proteobacteria, *Pseudomonas*, *Sphingomonas* and *Enterobacteriaceae*.

In our study, 106 OTUs were annotated as members of *Xanthomonadales* and 42 as *Pseudomonadales*. Out of these, 40 *Xanthomonadales* OTUs and 24 *Pseudomonadales* OTUs appeared to be unique to the *P. abies* wood samples and were more abundant in south- than in north-exposed wood samples. Kielak and colleagues (2016) found that the early stage of *Pinus sylvestris* wood decay was dominated by these two bacterial groups which are known for their fast growth and high metabolic versatility, and have been found to be associated with wood-feeding beetle larvae (Reid *et al.*, 2011). Hervé and colleagues (2014) also observed that *Xanthomonadaceae* was one of the most abundant bacterial families detected by pyrosequencing in *F. sylvatica* deadwood. Indeed, members of this family have previously been found to be strongly associated with decaying wood under both field and laboratory conditions (Folman *et al.*, 2008; Zhang *et al.*, 2008; Valášková *et al.*, 2008), regardless of the host-tree specificity (Hervé *et al.*, 2016). While in our study, *Xanthomonadales* seemed to be linked to early decay stages, there was no time effect on the presence of *Pseudomonadales* OTUs, which is in disagreement with Sun and colleagues (2014) who reported that the successional abundance of *Pseudomonas* decreased with incubation time.

Due to low nitrogen availability in deadwood it has been hypothesised that wood-inhabiting fungi might benefit from associations with nitrogen-fixing bacteria to meet their nitrogen requirements for vegetative and generative growth (Merrill and Cowling, 1966; Johnston *et al.*, 2016). Hoppe and colleagues (2015) reported that diazotrophic *Alphaproteobacteria* (*Rhizobiales*) accounted for up to 25% of the bacterial community in *P. abies* logs during the intermediate and advanced stages of decay. Although in our study they accounted for a smaller percentage (altogether 10% of all reads), 206 different *Rhizobiales* OTUs were detected. Hoppe and colleagues (2015) found that the most abundant OTU was assigned to the genus *Methylovirgula*, which has been shown to contain the *nifH* gene. Likewise, Kielak and colleagues (2016) also detected a higher abundance of these potential nitrogen-fixing candidates (*Rhizobiales*, *Methylovirgula*) at the middle and late stages, even though they did not constitute the dominant groups in the overall community. Although *Methylovirga* was detected in our experimental *P. abies* wood blocks, their number and abundance was low compared with previous studies. Despite the fact that many OTUs could not be assigned at the genus level, we found that the largest *Rhizobiales* OTUs were identified as *Bradyrhizobium* (3.5%)*, Rhizobium* (1.2%) and *Tardiphaga* (0.6%). While the abundance of *Bradyrhizobium*

was higher in soil, *Tardiphaga* was more abundant in wood; and, in general, the abundance of *Rhizobiales* OTUs increased in the *P. abies* wood blocks as decay progressed ($p < 2.2e\text{-}16$). We hypothesise that the underlying soil influenced which bacterial species were able to thrive in the exposed wood blocks as the majority of *Rhizobiales* OTUs were detected in both wood and soil samples (152 out of 206 OTUs).

Bacteria belonging to *Burkholderiales* have also been shown to be capable of nitrogen-fixation and efficiently degrade cellulose and aromatic compounds (Štursová *et al.*, 2012). All these features suggest that *Burkholderia* might play a relevant role during wood decay as previously pointed out by Sun and colleagues (2014) and Kielak and colleagues (2016). *Burkholderiales* OTUs found in our dataset were numerous (238 OTUs), diverse and accounted for more than 10% of all reads. The genera *Burkholderia* (62 OTUs)*, Naxibacter* (31 OTUs) and *Massilia* (7 OTUs) were frequently detected. Many OTUs belonged to the families *Oxalobacteraceae* and *Comamonadaceae.* In contrast to other studies (Sun *et al.*, 2014; Hoppe *et al.*, 2015), *Burkholderiales* were on average more abundant in the earlier stages of *P. abies* decay ($p = 0.008$). Interestingly, there were more *Burkholderiales* OTUs in the wood compared with the soil samples (85 OTUs unique to wood, 22 OTUs unique to soil), but the abundance of *Burkholderiales* OTUs was by trend higher in the soil samples ($p = 0.056$), because the abundant *Burkholderiales* OTUs were overrepresented in soil.

Concluding, the study reveals a high and exposure-dependent diversity of bacteria in *P. abies* deadwood at the initial stage of decay. The strong correlation to both the environment and between bacterial OTUs points toward an underestimated role of bacteria in deadwood decay, including polymer-degrading bacteria and nitrogen-fixing bacteria as potential north-suppliers for fungal deadwood decomposers; therefore, especially the interaction of bacterial and fungal deadwood colonizers needs further investigation to untangle possible cross-kingdom competition and promotion. As many OTUs could not be assigned at the genus level and little genetic and metabolic information is available in the databases, isolation studies are urgently needed to further identify the functional potential and role of these unannotated bacteria in the overall deadwood decay dynamics in forest ecosystems.

Experimental procedures

Study area and experimental set-up

The study sites were located at similar altitudes, that is at 1930 and 1995 m a.s.l. at the north- and the south-facing slope, respectively, in the European Alps (Val di Rabbi,

Trentino, northern Italy). They are part of an observation network with a comprehensive characterization of the soils (Egli *et al.*, 2006; Bardelli *et al.*, 2017), which are classified as Episkeletic Podzol and Skeletic Umbrisol. The mean annual temperature ranges from 8.2°C at the valley floor (about 750 m a.s.l.) to about 0°C at 2300 m a. s.l., and the mean annual precipitation ranges from 800 to 1300 mm (Sboarina and Cescatti, 2004).

At each study site a field experiment using soil meso-cosms was set up as described in Fravolini and colleagues (2016). Mesocosms (∅ 10.2 cm and 25 cm long PVC tubes) were installed into the soil in the summer of 2012 and placed > 1 m from large trees and > 0.5 m from adjacent mesocosms, leaving a rim of about 1 cm at the surface. Briefly, before the experiment started, the equally sized (5 cm × 5 cm × 2 cm) wood blocks were cut from the same log of one single forest tree growing in the same region where the experiment was conducted. Until they were used in the mesocosms, the blocks were stored in a dry place at room temperature. All the wood blocks were equally treated and had similar compositions at t0 (mass (n = 50): 22.5 ± 3.1 g; volume (all blocks): 50 cm^3; density (n = 50): 0.5 ± 0.06 g/cm^3; humidity (n = 50): 8.2% ± 2.01%; content of cellulose (n = 5): 44.5% ± 4.53%; content of Klason lig-nin (n = 5): 30.4% ± 1.47%; content of total lignin (n = 5): 30.7% ± 1.49%). For molecular analysis, three wood blocks were initially kept as controls and referred to as t0. Soil sam-ples (n = 3; t0) were also collected in the surrounding area of the mesocosms set up at both north- and south-facing sites directly before placing the wood blocks. Initiating the experiment, the wood blocks of Norway spruce [*Picea abies* (L.) Karst] were placed on top of the soil mesocoms 1 year later (June 2013) and covered with the original top-soil cover (Supporting Information Fig. S10). After 12 (t1), 25 (t2), 52 (t3) and 104 (t4) weeks the mesocosms, that is the wood blocks and the uppermost topsoil layer (0–5 cm), were destructively sampled (three replicate mesocosms for each time point). The top 5 cm refers to the soil fraction that was in direct contact with the wood blocks from the very beginning of the experiment. All the samples were placed into polyethylene bags and transported on ice to the labora-tory. The wood blocks were air-dried at room temperature in an incubator for a couple of hours and the entire wood block was cut-milled (4 mm; Fritsch-Pulverisette) to perform all the analyses on the very same homogenous sample. The soil was sieved (< 2 mm) and samples were stored at −20°C upon analyses.

Physico-chemical parameters

The moisture content of wood and soil samples was determined by oven-drying for 24 h at 105°C. The pH was determined from water extracts (1:5 and 1:10, w/v for soil and wood, respectively) by using a pH meter

Metrohm 744. The α-cellulose content from the wood blocks was assessed following the protocol of Leavitt and Danzer (1993) and Boettger and colleagues (2007).

DNA extraction

Total DNA was extracted from soil (0.2 g fresh weight, fw) and wood samples (0.1 g fw) by using commercial kits (MP, Biomedicals), FastDNA™ SPIN Kit for soil and FastDNA® Kit, respectively, in combination with the Fast DNA Instrument as described in Ascher and colleagues (2009). In the case of wood samples, one ¼ ceramic sphere (MP Biomedicals cat # 6540–424) was added to the lysing tubes. All DNA extracts were purified using the GeneClean procedure (Fast DNA™ SPIN Kit for soil).

Illumina MiSeq sequencing and bioinformatics pipeline

Bacterial communities were assessed by sequencing of the V3–4 region of the 16S rRNA gene using the primer pair 341F/802R (Lladó *et al.*, 2015) on an Illumina MiSeq flowcell using the 2 × 250 bp paired-end approach (Microsynth AG, Switzerland).

The analysis of raw data (PRJNA427454) was per-formed in Mothur v.1.37.6 (Schloss *et al.*, 2009). Samples contained 80,000 ±33,000 reads on average after quality filtering (trimming, primer removal) and the merging of forward and reverse reads. PCR and sequencing errors were removed following MiSeq SOP (Kozich *et al.*, 2013). Briefly, sequences were screened (max length of 300 bp, min length of 230 bp, no ambiguities and max homopolymer of 8 nucleotides) and unique sequences were aligned to the SILVA database (release 102) (Yilmaz *et al.*, 2014). Chimeric sequences were removed using UCHIME (Edgar *et al.*, 2011) implemented in Mothur. After preclustering (using diffs = 4), operational taxonomic units (OTUs) were generated on 97% similar-ity. After removing those OTUs < 5 reads, the final OTU table was subsampled to the smallest sample size (30 001 reads per sample). Sequences and OTUs were classified using the RDP trainset reference database (Wang *et al.*, 2007) applying a cut-off of 80. Alpha diver-sity (richness, Chao, Shannon index, shared Chao and rarefaction curves) was analysed in Mothur. The sub-sampled OTU table was used for all data analysis.

Statistical analyses

Non-metric multidimensional scaling (NMDS) was per-formed in R 3.2.5 (R Core Team) using the package vegan (Oksanen *et al.*, 2016) based on Bray–Curtis dis-similarity. Permutational multivariate analysis of variance (McArdle and Anderson, 2001) was used to model the influence of the experimental factors on the dissimilarity

matrix using the Adonis function of vegan. The within group homogeneity of sample groups was estimated in dependence of the time and the exposure as distance to centroid using the betadisper function in vegan. Pielous' evenness was calculated as Shannon index/log (richness).

The effect of both the time and the exposure on the ratio between richness and diversity was modelled using a linear approach by predicting the ratio in dependence of the time and the exposure as factorized variables. The relative contribution of the factor coefficient to the total sum of squares (SS) was used to standardize size effects. Effects were considered significant at a confidence interval of 95%.

Environmental variables were correlated on the ordination using functions envfit and bioenv in vegan. Variables (moisture, cellulose and pH) with significant impact on the ordination were then correlated with all the OTUs in the dataset using the Spearman correlation. OTUs with a correlation coefficient > 0.5 were further investigated. Overrepresented OTUs in different sample groups were identified using LEfSe (Segata *et al.*, 2011) implemented in Mothur. Only OTUs with a linear discriminant analyses (LDA) log (score) > 3 and a significance within 95% confidence interval were considered for further investigation. Correlations between OTUs present in at least three samples were analysed applying Pearson correlation coefficient. The correlation matrix was visualized in R using igraph package (Csardi and Nepusz, 2006). Wilcoxon rank sum test was applied to determine if two samples differed. Differences were considered significant at a confidence level of 95% ($p < 0.05$). Figures were produced in R, partially applying ggplot2 package (Wickham, 2009).

Acknowledgements

References

Ascher, J., Ceccherini, M. T., Pantani, O. L., Agnelli, A., Borgogni, F., Guerri, G., *et al.* (2009) Sequential extraction and genetic fingerprinting of a forest soil metagenome *Appl Soil Ecol*. **42**: 176–181.

Baas Becking, L. (1931) *Gaia of Leven en Aarde.* The Hague: Martinus Nijhoff.

Bardelli, T., Gómez-Brandón, M., Ascher-Jenull, J., Fornasier, F., Arfaioli, P., Francioli, D., *et al.* (2017) Effects of slope exposure on soil physico-chemical and microbiological properties along an altitudinal climosequence in the Italian alps *Sci Total Environ*. **575**: 1041–1055.

Beijerinck, M. W. (ed). (1913) *Jaarboek van de Koninklijke Akademie van Wetenschappen. De infusies en de ontdekking der bakterien*. Amsterdam: C. van der Post.

Boettger, T., Haupt, M., Knoller, K., Weise, S. M., Waterhouse, J. S., Rinne, K. T., *et al.* (2007) Wood cellulose preparation methods and mass spectrometric analyses of $\delta^{13}C$, $\delta^{18}O$, and nonexchangeable delta H_{-2} values in cellulose, sugar, and starch: an interlaboratory comparison *Anal Chem*. **79**: 4603–4612.

Brown, M. E., and Chang, M. C. (2014) Exploring bacterial lignin degradation *Curr Opin Chem Biol*. **19**: 1–7.

Chang, C., Wu, F., Yang, W., Xu, Z., Cao, R., He, W., *et al.* (2017) The microbial community in decaying fallen logs varies with critical period in an alpine forest *PLOS One.* **12**: e0182576. https://doi.org/10.1371/journal.pone.0182576.

Csardi, G., and Nepusz, T. (2006). The igraph software package for complex network research. *Int J Complex Syst* **1695**: 1–9. http://igraph.org.

DeAngelis, K. M., Allgaier, M., Chavarria, Y., Fortney, J. L., Hugenholtz, P., Simmons, B., *et al.* (2011) Characterization of trapped lignin-degrading microbes in tropical forest soil *PLOS One*. **6**: e19306. https://doi.org/10.1371/journal.pone.0019306.

Edgar, R. C., Haas, B. J., Clemente, J. C., Quince, C., and Knight, R. (2011) UCHIME improves sensitivity and speed of chimera detection *Bioinformatics*. **27**: 2194–2200.

Egli, M., Mirabella, A., Sartori, G., Zanelli, R., and Bischof, S. (2006) Effect of north and south exposure on weathering rates and clay mineral formation in alpine soils *Catena*. **67**: 155–174.

Egli, M., Hafner, S., Derungs, C., Ascher-Jenull, J., Camin, F., Sartori, G., *et al.* (2016) Decomposition and stabilisation of Norway spruce needle-derived material in alpine soils using a ^{13}C-labelling approach in the field *Biogeochem*. **131**: 321–338.

Fagervold, S. K., Romano, C., Kalenitchenko, D., Borowski, C., Nunes-Jorge, A., Martin, D., and Galand, P. E. (2014) Microbial communities in sunken wood are structured by wood-boring bivalves and location in a submarine canyon *PLOS One*. **9**: e96248. https://doi.org/10.1371/journal.pone.0096248.

Folman, L. B., Gunnewiek, P., Boddy, L., and de Boer, W. (2008) Impact of white-rot fungi on numbers and community composition of bacteria colonizing beech wood from forest soil *FEMS Microbiol Ecol*. **63**: 181–191.

Fravolini, G., Egli, M., Derungs, C., Cherubini, P., Ascher-Jenull, J., Gómez-Brandón, M., *et al.* (2016) Soil attributes and microclimate are important drivers of initial deadwood decay in sub-alpine Norway spruce forests *Sci Total Environ*. **569-570**: 1064–1076.

Garbarino, M., Marzano, R., Shaw, J. D., and Long, J. N. (2015) Environmental drivers of deadwood dynamics in woodlands and forests *Ecosphere*. **6**: 1–24.

Gómez-Brandón, M., Ascher-Jenull, J., Bardelli, T., Fornasier, F., Fravolini, G., Arfaioli, P., *et al.* (2017) Physico-chemical and microbiological evidence of exposure effects on *Picea abies* – coarse woody debris at different stages of decay *For Ecol Manage*. **391**: 376–389.

Hervé, V., Le Roux, X., Uroz, S., Gelhaye, E., and Frey-Klett, P. (2014) Diversity and structure of bacterial communities associated with Phanerochaete chrysosporium during wood decay *Environ Microbiol*. **16**: 2238–2252.

Hervé, V., Ketter, E., Pierrat, J. C., Gelhaye, E., and Frey-Klett, P. (2016) Impact of *Phanerochaete chrysosporium* on the functional diversity of bacterial communities associated with decaying wood *PLOS One*. **11**: e0147100. https://doi.org/10.1371/journal.pone.0147100.

Hoppe, B., Krüger, D., Kahl, T., Arnstadt, T., Buscot, F., Bauhus, F., *et al.* (2015) A pyrosequencing insight into sprawling bacterial diversity and community dynamics in decaying deadwood logs of *Fagus sylvatica* and *Picea abies Sci Rep*. **5**: 9456.

Johnston, S. R., Boddy, L., and Weightman, A. J. (2016) Bacteria in decomposing wood and their interactions with wood-decay fungi *FEMS Microbiol Ecol*. **92**: 1–12.

Kielak, A. M., Scheublin, T. R., Mendes, L. W., van Veen, J. A., and Kuramae, E. E. (2016) Bacterial community succession in pine-wood decomposition *Front Microbiol*. **7**: 1–12.

Kozich, J. J., Westcott, S. L., Baxter, N. T., Highlander, S. K., and Schloss, P. D. (2013) Development of a dual-index sequencing strategy and curation pipeline for analyzing amplicon sequence data on the MiSeq Illumina sequencing platform *Appl Environ Microbiol*. **79**: 5112–5120.

Leavitt, S. W., and Danzer, S. R. (1993) Method for batch processing small wood samples to holocellulose for stable-carbon isotope analysis *Anal Chem*. **65**: 87–89.

Lladó, S., Covino, S., Solanas, A. M., Petruccioli, M., D'Annibale, A., and Vinas, M. (2015) Pyrosequencing reveals the effect of mobilizing agents and lignocellulosic substrate amendment on microbial community composition in a real industrial PAH-polluted soil *J Hazard Mater*. **283**: 35–43.

Lladó, S., Zifčákovâ, L., Vetrovsky, T., Eichlerová, I., and Baldrian, P. (2016) Functional screening of abundant bacteria from acidic forest soil indicates the metabolic potential of Acidobacteria subdivision 1 for polysaccharide decomposition *Biol Fert Soils*. **52**: 251–260.

Lynch, J., Benedetti, A., Insam, H., Smalla, C., Torsvik, V., Nuti, M., and Nannipieri, P. (2004) Microbial diversity in soil: ecological theories, the contribution of molecular techniques and the impact of transgenic plants and transgenic microorganisms – a review *Biol Fertil Soils*. **40**: 363–385.

Mäkipää, R. T., Schigel, D., Rinne, K. T., Pennanen, T., Abrego, N., *et al.* (2017) Interactions between soil- and dead wood-inhabiting fungal communities during the decay of Norway spruce logs *ISME J*. **11**: 1964–1974.

McArdle, B. H., and Anderson, M. J. (2001) Fitting multivariate models to community data: a comment on distance-based redundancy analysis *Ecology*. **82**: 290–297.

Merrill, W., and Cowling, E. B. (1966) Role of nitrogen in wood deterioration: amounts and distribution of nitrogen in tree stems *Can J Bot*. **44**: 1555–1580.

Mikkelson, G. M., McGill, B. J., Beaulieu, S., and Beukema, P. L. (2011) Multiple links between species diversity and temporal stability in bird communities across North America *Evol Ecol Res*. **13**: 361–372.

Nagler, M., Ascher, J., Gómez-Brandón, M., and Insam, H. (2016) Soil microbial communities along the route of a venturous cycling trip *Appl Soil Ecol*. **99**: 13–18.

Oksanen, J., Blanchet, G.F., Kindt, R., Legendre, P., Minchin, P.R., O'Hara, R.B., *et al.* (2016). Vegan: community ecology package. R package version 2 3. https://CRAN.R-project.org/package=vegan.

Pan, Y., Birdsey, R. A., Fang, J., Houghton, R., Kauppi, P. E., Kurz, W. A., *et al.* (2011) A large and persistent carbon sink in the world's forests *Science*. **333**: 988–993.

Pandit, S. N., Kolasa, J., and Cottenie, K. (2009) Contrasts between habitat generalists and specialists: an empirical extension to the basic metacommunity framework *Ecology*. **90**: 2253–2262.

Reid, N., Addison, S. L., Mcdonald, L. J., and Lloyd-Jones, G. (2011) Biodiversity of active and inactive bacteria in the gut flora of wood-feeding huhu bettle larvae (*Prionoplus reticularis*) *Appl Environ Microbiol*. **77**: 7000–7006.

Rinta-Kanto, J. M., Sinkko, H., Rajala, T., Al-Soud, W. A., Sørensen, S. J., Tamminen, M. V., *et al.* (2016) Natural decay process affects the abundance and community structure of bacteria and Archaea in *Picea abies* logs *FEMS Microbiol Ecol*. **92**: fiw087.

Sboarina, C., and Cescatti, A. (2004). Il clima del Trentino – distribuzione spaziale delle principali variabili climatiche [The climate of Trentino – spatial distribution of the principal climatic variables]. Report 33, Centro di Ecologia Alpina Monte Bondone, Trento, Italy, p. 20.

Schloss, P. D., Westcott, S. L., Ryabin, T., Hall, J. R., Hartmann, M., Hollister, E. B., *et al.* (2009) Introducing mothur: open-source, platform-independent, community-supported software for describing and comparing microbial communities *Appl Environ Microbiol*. **75**: 7537–7754.

Segata, N., Izard, J., Waldron, L., Gevers, D., Miropolsky, L., Garret, W. S., *et al.* (2011) Metagenomic biomarker discovery and explanation *Genome Biol*. **12**: R60.

Stokland, Y. N., Siitonen, J., and Jonsson, B. G. (2012) *Biodiversity in Dead Wood*. London: Academic Press.

Štursová, M., Zifčákováâ, L., Leigh, M. B., Burgess, R., and Baldrian, P. (2012) Cellulose utilization in forest litter and soil: identification of bacterial and fungal decomposers *FEMS Microbiol Ecol*. **80**: 735–746.

Stutz, K. P., and Lang, F. (2017) Potentials and unknowns in managing coarse woody debris for soil functioning *Forests*. **8**: 37. https://doi.org/10.3390/f8020037.

Sun, H., Terhonen, E., Kasanen, R., and Asiegbu, F. O. (2014) Diversity and community structure of primary wood-inhabiting bacteria in boreal forest *Geomicrobiol J*. **31**: 315–324.

Thibaut, L. M., Connolly, S. R., and He, F. (2013) Understanding diversity-stability relationships: towards a unified model of portfolio effects *Ecol Lett*. **16**: 140–150.

Tláskal, V., Vorísková, J., and Baldrian, P. (2016) Bacterial succession on decomposing leaf litter exhibits a specific

occurrence pattern of cellulolytic taxa and potential decomposers of fungal mycelia *FEMS Microbiol Ecol*. **92**: 1–9.

Tláskal, V., Zrustová, P., Vrska, T., and Baldrian, P. (2017). Bacteria associated with decomposing dead wood in a natural temperate forest. *FEMS Microbiol Ecol* **93**: fix 157. doi: https://doi.org/10.1093/femsec/fix157

Valášková, V., de Boer, W., Gunnewiek, P. J., Pospísek, M., and Baldrian, P. (2008) Phylogenetic composition and properties of bacteria coexisting with the fungus Hypholoma fasciculare in decaying wood *ISME J*. **3**: 1218–1221.

Wang, Q., Garrity, G. M., Tiedjy, J. M., and Cole, J. R. (2007) Naïve Bayesian classifier for rapid assignment of rRNA sequences into the new bacterial taxonomy *Appl Env Microbiol*. **73**: 5261–5267.

Wickham, H. (2009) *Ggplot2: Elegant Graphics for Data Analysis*. New York: Springer Verlag.

Wittebolle, L., Marzorati, M., Clement, L., Balloi, A., Daffonchio, D., Heylen, K., *et al*. (2009) Initial community evenness favours functionality under selective stress *Nat Lett*. **458**: 623–626.

Yilmaz, P., Parfrey, L., Yarza, P., Gerken, J., Pruesse, E., Quast, C., *et al*. (2014) The SILVA and 'all-species living tree project (LTP)' taxonomic frameworks *Nucleic Acids Res*. **42**: 643–648.

Youssef, N. H., and Elshahed, M. S. (2014) The phylum Planctomycetes . In *The Prokaryotes: Other Major Lineages of Bacteria and the Archaea*. Rosenberg, E., DeLong, E. F., Lory, S., Stackebrandt, E., Thompson, F. (eds). Berlin Heidelberg: Springer, pp. 759–810.

Zhang, H. B., Yang, M. X., and Tu, R. (2008) Unexpectedly high bacterial diversity in decaying wood of a conifer as revealed by a molecular method *Int Biodeterior Biodegrad*. **62**: 471–474.

Supporting Information

Additional Supporting Information may be found in the online version of this article at the publisher's web-site:

Fig. S1. Rarefaction curves of bacterial community data obtained by Illumina Miseq profiling. Plots A and C display measures of the *P. abies* wood block samples and plots B and D display measures for the underlying soil samples. In plots A and B estimated richness calculated as Chao index was sampled. Plots C and D show the actual measured richness of each sample, expressed as how many OTUs were detected given a certain number of sequences sampled.

Fig. S2. Abiotic characteristics of the *P. abies* wood blocks after 12 (t1), 25 (t2), 52 (t3) and 104 (t4) weeks of incubation (*in-field* mesocosms) at the north (N)- and the south (S)- facing slopes. Upper left: moisture content. Upper right: pH. Lower left: Klason lignin determined according to Dence and Lin (1992). Lower right: cellulose concentration. Data points with 'NS' exposure indicate sampling point t0 where wood blocks have not yet been exposed.

Fig. S3. Abiotic soil characteristics at the north (N)- and the south (S)- facing slopes after 12 (t1), 25 (t2), 52 (t3) and 104 (t4) weeks of incubation (*in-field* mesocosms). Upper left: moisture content. Upper right: pH. Lower left: total carbon content. Lower right: total nitrogen content. Total carbon and nitrogen contents were analysed in oven-dried samples by using a CHN-analyser (TruSpec CHN Makro/LECO).

Fig. S4. Decorana analysis of bacterial community data obtained by Illumina Miseq profiling. Multidimensional character of bacterial OTU data was detrended and compressed into two dimensions based on Bray Curtis measure. The influence of rare OTUs on the ordination was downweighted during analysis. Four axes were retained. Site scores were coloured according to substrate with grey circles indicating soil and brown circles indicating deadwood samples. Shades of brown indicate north- (light) and south- (dark) exposure for wood samples. Sample groups according to the experimental factors were drawn for north- and south-exposure for soil samples and decay time for deadwood samples. Ellipses embracing sample groups were drawn at a confidence interval of 95% around group centroid. Wood samples prior to application to the *in-field* mesocosms (t0) are coloured in black.

Fig. S5. Abundances and number of OTUs at phylum level according to sample groups. Abundances based on subsampled, normalized read abundance were averaged across sample groups giving major effect of substrate (A) and exposure on soil samples (B). For wood samples, the decay is a function of exposure and time (C). The subfigure (D) displays the taxonomic classification of only OTUs unique to wood sample groups. The subfigure E illustrates the phylum distribution of only OTUs correlating to an environmental parameter (with the absolute value of Spearman's rho > 0.5). Subfigure *F* illustrates the phylum distribution of OTUs correlating to OTUs characteristic to a wood sample group (left part of the subfigure) and the phylum distribution of OTUs correlating to big OTUs (read amount > 0.5% of total reads within the dataset) and highly correlated OTUs [more than 100 connections in the correlation network (Fig. 5 and Supporting Information Fig. S6)]. Terminology: *Freq.* before a category (x axis) indicates that the number of OTUs within a phylum is given, independent of the OTUs' abundance. *Mean.* indicates the numeric mean of abundances across samples. *Unique.* implies that only OTUs absent in all other sites are displayed. *Total.* implies that all of the OTUs (independent of sample groups) are displayed. *Normal.* For better comparability, the phylum distribution of all OTUs in the dataset is displayed. Deviations from this distribution might be interpreted as deviations from the expected distribution.

Fig. S6. Physicochemical decay characteristics of *P. abies* wood blocks as originally published by Fravolini and colleagues (2016)**.** (Left) Weight (±standard error) of the wood blocks (placed into mesocosms) as a function of time (0–2 years), site (altitude) and exposure (north vs. south). (Middle) Amount of cellulose (=concentration × dry weight of wood block; weight ± standard error) as a function of time (0–2 years), site (altitude) and exposure (north vs. south). (Right) Amount of lignin (=concentration × dry weight of wood block; weight ± standard error) in the wood blocks as a function of time (0–2 years), site (altitude) and exposure (north vs. south).

Fig. S7. Fungal 18S gene copy numbers (GCN) per gram of dried weight according to Bardelli *et al*. (2017)**.** The abundances of fungi in the wood and soil samples were observed by the copy numbers of the fungal 18S rRNA gene quantified

by qPCR. Differences were analysed by Wilcoxon rang sum test. (A) Fungal GCN differed between wood and soil samples (p = 1.9e-10). (B) Fungal GCN did not differ between north- and south-exposed soil. (C) Fungal GCN did not differ between time points. (D) Fungal GCN did not differ between north- and south- exposed wood blocks. (NS refers to t0, because at this time point, the wood blocks have not been exposed, yet.) (E) Fungal GCN increased from t0 to early time points (p = 0.004) and remained stable until the end of the observation period.

Fig. S8. Correlation of wood OTUs to the environmental variables of the wood blocks. The abundances of OTUs present in at least three wood samples were correlated to the environmental variables moisture content, cellulose content and pH. Significant correlations above |rho > 0.5| were considered of ecological interest. The plot displays the distribution of correlation coefficients of the wood OTUs indicating the association of the correlating OTU to a certain sampling point or slope exposure. OTUs were associated to sample groups by being either unique, characteristic [defined as significantly overrepresented in one sample group as determined by linear discriminant analysis size effect (LEfSe) algorithm (Segata *et al.*, 2011) (LDA > 3, p < 0.05)] or not associated (shared).

Fig. S9. Correlation network of bacterial OTUs identified by Illumina Miseq profiling in both *P. abies* wood blocks and underlying soil. Correlations were calculated as Pearson's correlation on all OTUs in the dataset which were found in at least three samples. Only correlations above a set threshold were kept in the networks. The two columns of networks display the very same network in each row. The left and right

columns indicate OTUs overrepresented or unique to north- and south-exposed *P. abies* respectively. The difference between rows (A–D) is the threshold set for a correlation between two OTUs in order to be ecologically meaningful: (A) |r| > 0.6, (B) |r| > 0.7, (C) |r| = r > 0.8, (D) |r| = r > 0.9.

Fig. S10. Correlation network of selected bacterial OTUs identified by Illumina Miseq profiling in both *P. abies* wood blocks and underlying soil. In the network lines connect OTUs indicating that the abundances of these OTUs correlate above a set threshold of r > 0.8, assuming that these OTU correlations were of ecologically meaningful co-occurrences. Correlations were calculated as Pearson's correlation on all OTUs in the dataset, which were present in at least three independent samples. The picture drawn for the integration (degree of connectivity) of OTUs characteristic for *P. abies* wood blocks decay on north- (squares) and south- (circles) facing slopes, was comparable across correlation coefficient thresholds ranging from |r| > 0.6 to |r| = r > 0.9 (see also Supporting Information Fig. S9).

Fig. S11. Setup of the mesocosm experiment: Wood blocks were covered with the original topsoil cover. At the north- and the south-facing site a field experiment using soil mesocosms was set up as described in Fravolini and colleagues (2016). Mesocosms (∅ 10.2 cm and 25 cm long PVC tubes) were installed into the soil in the summer of 2012 and placed >1 m from large trees and > 0.5 m from adjacent mesocosms, leaving a rim of about 1 cm at the surface. Equally sized (5 cm × 5 cm × 2 cm) wood blocks of Norway spruce [*Picea abies* (L.) Karst] were placed on top of the soil mesocoms 1 year later (June 2013) and were covered with the original topsoil cover.